

---

# One Risk to Rule Them All: A Risk-Sensitive Perspective on Model-Based Offline Reinforcement Learning

---

Marc Rigter<sup>1</sup> Bruno Lacerda<sup>1</sup> Nick Hawes<sup>1</sup>

## Abstract

Offline reinforcement learning (RL) is suitable for safety-critical domains where online exploration is too costly or dangerous. In safety-critical settings, decision-making should take into consideration the risk of catastrophic outcomes. In other words, decision-making should be *risk-sensitive*. Previous works on risk in offline RL combine together offline RL techniques, to avoid distributional shift, with risk-sensitive RL algorithms, to achieve risk-sensitivity. In this work, we propose risk-sensitivity as a mechanism to jointly address both of these issues. Our model-based approach is risk-averse to both epistemic and aleatoric uncertainty. Risk-aversion to epistemic uncertainty prevents distributional shift, as areas not covered by the dataset have high epistemic uncertainty. Risk-aversion to aleatoric uncertainty discourages actions that may result in poor outcomes due to environment stochasticity. Our experiments show that our algorithm achieves competitive performance on deterministic benchmarks, and outperforms existing approaches for risk-sensitive objectives in stochastic domains.

## 1. Introduction

In safety-critical applications, reinforcement learning (RL) is impractical due to the requirement for extensive random exploration that may be dangerous or costly. To alleviate this issue, offline (or batch) RL considers finding the best possible policy from pre-collected data. In safety-critical settings we wish to take into consideration the risk of catastrophic outcomes. In other words, we want decision-making to be *risk-sensitive*. However, the vast majority of offline RL research considers the expected value objective, and therefore disregards variability in performance between episodes.

One of the core issues in offline RL is avoiding distribu-

tional shift: to obtain a performant policy, we must ensure that the distribution of state-action pairs generated by the policy remains near the distribution covered by the dataset. Another way that we can view this is that we want the policy to be averse to *epistemic* uncertainty (uncertainty stemming from a lack of data). In regions not covered by the dataset, epistemic uncertainty is high and there will be large errors in the model or value function that may be exploited by the policy, resulting in the policy choosing erroneous actions.

In risk-sensitive RL, the focus is typically on finding policies that are risk-averse to environment stochasticity, i.e. *aleatoric* uncertainty. Previous approaches to risk-sensitive offline RL (Ma et al., 2021; Urpí et al., 2021) combine together two techniques: offline RL techniques, to avoid distributional shift; and risk-sensitive RL algorithms, to achieve risk-sensitivity. In other words, the issues of epistemic and aleatoric uncertainty are handled separately, using different techniques. In contrast, we propose to avoid epistemic uncertainty due to distributional shift, as well as aleatoric uncertainty due to environment stochasticity, by computing a policy that is risk-averse to both sources of uncertainty.

In this work we propose 1R2R, a model-based algorithm for risk-sensitive offline RL. We provide a new perspective by proposing to jointly optimise for risk-sensitivity towards both epistemic and aleatoric uncertainty. The intuition behind our approach is that we should optimise the policy so that it avoids the risk of a bad outcome *either* due to high uncertainty in the model (epistemic uncertainty) or due to randomness in the environment (aleatoric uncertainty). Unlike previous approaches to risk-sensitive offline RL (Urpí et al., 2021; Ma et al., 2021) which combine offline RL techniques with risk-sensitive optimisation, our approach modifies standard RL methods *only by considering risk*. Therefore, our approach is conceptually simpler than existing approaches. Our main contributions are:

- Proposing risk-sensitivity towards epistemic uncertainty as a mechanism to address the issue of distributional shift in offline RL.
- Introducing the first model-based algorithm for risk-sensitive offline RL, which jointly addresses epistemic and aleatoric uncertainty.

In our experiments, we evaluate our approach in several sce-

---

<sup>1</sup>Oxford Robotics Institute, University of Oxford. Correspondence to: Marc Rigter <mrigter@robots.ox.ac.uk>.

narios. Our experiments show that our algorithm achieves competitive performance relative to state-of-the-art baselines on deterministic benchmarks (Fu et al., 2020), and outperforms existing approaches for risk-sensitive objectives in stochastic domains.

## 2. Related Work

**Offline RL:** Offline RL addresses the problem of learning policies from fixed datasets, and has been applied to domains such as robotics (Zhou et al., 2022) and healthcare (Nie et al., 2021). Most works on offline RL are *risk-neutral*, meaning that they optimise expected value, the standard objective in sequential decision-making under uncertainty (Puterman, 2014). A key issue in offline RL is avoiding distributional shift so that the states visited by the learnt policy remain within the distribution covered by the dataset (Levine et al., 2020). Failing to mitigate this issue can lead to the policy learning to visit out-of-distribution states to exploit errors in the value function (Kumar et al., 2019) or model (Kidambi et al., 2020), and as a result, the policy may perform poorly on the real environment.

Model-free approaches to offline RL do not require a learnt model. Approaches for model-free offline RL include: constraining the learnt policy to be similar to the behaviour policy (Fujimoto et al., 2019; Kostrikov et al., 2022; Wu et al., 2019; Fujimoto & Gu, 2021), conservative value function updates (Cheng et al., 2022; Kostrikov et al., 2021; Kumar et al., 2020; Xie et al., 2021), importance sampling algorithms (Liu et al., 2019; Nachum et al., 2019), or using Q-ensembles for more robust value estimates (Agarwal et al., 2020; An et al., 2021; Yang et al., 2022).

In contrast, model-based approaches learn a model of the environment and generate synthetic data from that model (Sutton, 1991) to optimise a policy via planning (Argenson & Dulac-Arnold, 2021) or RL algorithms (Kidambi et al., 2020; Yu et al., 2020; 2021). By training a policy on additional synthetic data, model-based approaches have the potential for broader generalisation (Ball et al., 2021). Approaches to preventing model exploitation include constraining the policy to be similar to the behaviour policy (Matsushima et al., 2021; Swazinna et al., 2021) or applying conservative value function updates (Yu et al., 2021) in the same fashion as model-free approaches. Another approach is to modify the learnt MDP by either applying reward penalties for state-action pairs with high uncertainty (Kidambi et al., 2020; Lu et al., 2022; Yang et al., 2021; Yu et al., 2020), or modifying the transition model to produce pessimistic synthetic transitions (Rigter et al., 2022b; Guo et al., 2022). Very recent work by Guo et al. (2022) biases sampling from the model in a pessimistic manner, and is the most similar existing algorithm to our work. However, unlike our work, Guo et al. (2022) does not consider risk.

**Risk-Sensitive RL:** Many previous works have argued for risk-sensitive algorithms in safety critical applications (Garcia & Fernández, 2015; Majumdar & Pavone, 2020). Risk-sensitive algorithms for MDPs include approaches that adapt policy gradients to risk-sensitive objectives (Chow et al., 2017; Tamar et al., 2012; 2015a;b), and methods based on value iteration (Ruszczyński, 2010; Chow et al., 2015). More recently, a number of works have utilised distributional RL (Bellemare et al., 2017; Morimura et al., 2010), which learns a distributional value function that predicts the full return distribution. Knowledge of the return distribution can then be used to optimise a risk-sensitive criterion (Dabney et al., 2018; Keramati et al., 2020; Ma et al., 2020). Most risk-sensitive RL algorithms are model-free, however model-based approaches which utilise model-predictive control have been also proposed (Webster & Flach, 2021; Zhang et al., 2020).

The main focus of research on risk-sensitive online RL is risk due to environment stochasticity (Eriksson & Dimitrakakis, 2020) (i.e. aleatoric uncertainty). However, there are a number of works that explicitly address risk due to epistemic uncertainty (Clements et al., 2020; Depeweg et al., 2018; Eriksson & Dimitrakakis, 2020; Eriksson et al., 2022; Rigter et al., 2021). To our knowledge, this is the first work to consider risk due to epistemic uncertainty as a means to mitigate distributional shift in offline RL.

**Risk-Sensitive Offline RL:** To our knowledge, there are two previous works that address risk-sensitive offline RL: ORAAC (Urpí et al., 2021) and CODAC (Ma et al., 2021). To avoid distributional shift, ORAAC utilises policy constraints, while CODAC employs pessimistic value function updates to penalise out-of-distribution state-action pairs. Both algorithms learn a distributional value function which is then used to optimise a policy for a risk-sensitive objective. Thus, both of these works are model-free, and combine techniques from offline RL and distributional RL, to address the issues of distributional shift and risk-sensitivity, respectively. In this work, we provide a new perspective by proposing to optimise for risk-sensitivity towards *both* epistemic uncertainty (stemming from distributional shift) and aleatoric uncertainty (stemming from environment stochasticity). Unlike previous approaches, our approach avoids the need to intermix different techniques, and is model-based.

## 3. Preliminaries

**MDPs and Offline RL:** An infinite-horizon MDP is defined by the tuple  $M = (S, A, T, R, s_0, \gamma)$ .  $S$  and  $A$  denote the state and action spaces respectively,  $R(s, a)$  is the reward function,  $T(s'|s, a)$  is the transition function,  $s_0$  is the initial state, and  $\gamma \in (0, 1)$  is the discount factor. In this work we consider deterministic Markovian policies,  $\pi \in \Pi$ , which

map each state to an action.

In offline RL we only have access to a fixed dataset of transitions from the MDP,  $\mathcal{D} = \{(s_i, a_i, r_i, s'_i)\}_{i=1}^{|\mathcal{D}|}$ . The goal of offline RL is to find a performant policy using the fixed dataset.

**Model-Based Offline RL Algorithms:** Model-based approaches to offline RL use a model of the MDP to help train a policy. The learnt dynamics model,  $\hat{T}$ , is typically trained via maximum likelihood estimation:  $\min_{\hat{T}} \mathbb{E}_{(s,a,s') \sim \mathcal{D}} [-\log \hat{T}(s'|s,a)]$ . A model of the reward function,  $\hat{R}(s,a)$ , can also be learnt if it is unknown. The estimated MDP,  $\hat{M} = (S, A, \hat{T}, \hat{R}, \mu_0, \gamma)$ , has the same state and action space as the true MDP but uses the learnt transition and reward functions. Thereafter, any planning or RL algorithm can be used to recover the optimal policy in the learnt model,  $\hat{\pi} = \arg \max_{\pi \in \Pi} J_{\hat{M}}^{\pi}$ . Here,  $J$  indicates the optimisation objective, which is typically the expected value of the discounted cumulative reward.

Unfortunately, directly applying this approach does not perform well in the offline setting due to distributional shift. In particular, if the dataset does not cover the entire state-action space, the model will inevitably be inaccurate for some state-action pairs. Thus, naive policy optimisation on a learnt model in the offline setting can result in *model exploitation* (Janner et al., 2019; Kurutach et al., 2018; Rajeswaran et al., 2020), i.e. the policy chooses actions that the model erroneously predicts will lead to high reward. In this work we propose to mitigate this issue by optimising a risk-averse policy.

Following previous works (Kidambi et al., 2020; Yu et al., 2021; 2020), we use model-based policy optimisation (MBPO) (Janner et al., 2019) to learn the optimal policy for  $\hat{M}$ . MBPO utilises a standard off-policy actor-critic RL algorithm. However, the value function is trained using an augmented dataset  $\mathcal{D} \cup \hat{\mathcal{D}}$ , where  $\hat{\mathcal{D}}$  is synthetic data generated by simulating rollouts in the learnt model. To generate the synthetic data, MBPO performs  $k$ -step rollouts in  $\hat{M}$  starting from states  $s \in \mathcal{D}$ , and adds this data to  $\hat{\mathcal{D}}$ . To train the policy, minibatches of data are drawn from  $\mathcal{D} \cup \hat{\mathcal{D}}$ , where each datapoint is sampled from the real data,  $\mathcal{D}$ , with probability  $f$ , and from  $\hat{\mathcal{D}}$  with probability  $1 - f$ .

**Risk Measures** We denote the set of all probability distributions by  $\mathcal{P}$ . Consider a probability space,  $(\Omega, \mathcal{F}, P)$ , where  $\Omega$  is the sample space,  $\mathcal{F}$  is the event space, and  $P \in \mathcal{P}$  is a probability distribution over  $\mathcal{F}$ . Let  $\mathcal{Z}$  be the set of all random variables defined over the probability space  $(\Omega, \mathcal{F}, P)$ . We will interpret a random variable  $Z \in \mathcal{Z}$  as a reward, i.e. the greater realisation of  $Z$ , the better. We denote a  $\xi$ -weighted expectation of  $Z$  by  $\mathbb{E}_{\xi}[Z] := \int_{\omega \in \Omega} P(\omega) \xi(\omega) Z(\omega) d\omega$ , where  $\xi : \Omega \rightarrow \mathbb{R}$  is a

function that re-weights the original distribution of  $Z$ .

A *risk measure* is a function,  $\rho : \mathcal{Z} \rightarrow \mathbb{R}$ , that maps any random variable  $Z$  to a real number. An important class of risk measures are *coherent* risk measures. These are risk measures that satisfy a set of properties that are consistent with rational risk assessments. A more detailed description and motivation for coherent risk measures is given by (Artzner et al., 1999; Majumdar & Pavone, 2020).

We will make use of two examples of coherent risk measures: the *conditional value at risk* (CVaR) (Rockafellar & Uryasev, 2002) and the *Wang risk measure* (Wang, 2000). For parameter  $\alpha$ , CVaR is the mean of the  $\alpha$ -portion of the worst outcomes:  $\rho_{\text{CVaR}}(Z, \alpha) = \mathbb{E}[z \sim Z \mid z \leq F_Z^{-1}(\alpha)]$ , where  $F_Z$  is the CDF of  $Z$ . For parameter  $\eta$ , the Wang risk measure for random variable  $Z$  can be defined as the expectation under a distorted cumulative distribution function  $\rho_{\text{Wang}}(Z, \eta) = \int_{-\infty}^{\infty} z \frac{\partial}{\partial z} g(F_Z(z)) dz$ , and the distortion function is  $g(\tau) = \Phi(\Phi^{-1}(\tau) + \eta)$ , where  $\Phi$  is the CDF of the standard normal distribution. In both instances, the parameters  $\alpha$  and  $\eta$  control the level of risk-aversion. We test our approach with these two risk measures because CVaR is commonly used and easy to interpret, but only considers the  $\alpha$ -portion of the distribution, while the Wang risk measure takes into consideration the entire distribution. However, the general approach we propose is compatible with any coherent risk measure.

All coherent risk measures can be represented using their dual representation (Artzner et al., 1999; Shapiro et al., 2021b). A risk measure,  $\rho$  is coherent if and only if there exists a convex bounded and closed set,  $\mathcal{B}_{\rho} \in \mathcal{P}$ , such that

$$\rho(Z) = \min_{\xi \in \mathcal{B}_{\rho}(P)} \mathbb{E}_{\xi}[Z] \quad (1)$$

Thus, the value of any coherent risk measure for any  $Z \in \mathcal{Z}$  can be viewed as an  $\xi$ -weighted expectation of  $Z$ , where  $\xi$  is the worst-case weighting function chosen from a suitably defined *risk envelope*,  $\mathcal{B}_{\rho}(P)$ . For more examples of coherent risk measures and their corresponding risk envelopes, we defer the reader to Shapiro et al. (2021b).

**Static and Dynamic Risk** In MDPs, the random variable of interest is usually the total reward received at each episode, i.e.  $Z_{\text{MDP}} = \sum_{t=0}^{\infty} \gamma R(s_t, a_t)$ . The *static* perspective on risk applies a risk measure directly to this random variable:  $\rho(Z_{\text{MDP}})$ . Thus, *static* risk does not take into account the temporal structure of the random variable in sequential problems, such as MDPs. This leads to the issue of “time inconsistency” (Boda & Filar, 2006). This means that if a certain action is considered less risky at one point in time, it might not be considered less risky at other points in time. This leads to non-Markovian optimal policies, and prohibits the straightforward application of dynamic programming due to the coupling of risk preferences over time.

This issue motivates *dynamic* risk measures, which take into consideration the sequential nature of the stochastic outcome, and are therefore time-consistent. Markov risk measures (Ruszczynski, 2010) are a class of dynamic risk which are obtained by recursively applying static coherent risk measures. Throughout this paper we will consider dynamic Markov risk over an infinite horizon, denoted by  $\rho_\infty$ . For policy  $\pi$ , MDP  $M$ , and static risk measure  $\rho$ , the corresponding Markov coherent risk  $\rho_\infty^\pi(M)$  is defined as

$$\rho_\infty^\pi(M) = R(s_0, \pi(s_0)) + \rho\left(\gamma R(s_1, \pi(s_1)) + \rho(\gamma^2 R(s_2, \pi(s_2)) + \dots)\right), \quad (2)$$

where  $\rho$  is a static coherent risk measure, and  $(s_0, s_1, s_2, \dots)$  indicates random trajectories drawn from the Markov chain induced by  $\pi$  in  $M$ . Note that in Eq. 2 the static risk measure is evaluated at each step according to the distribution over possible successor states.

We define the risk-sensitive value function under some policy  $\pi$  as:  $V^\pi(s) = \rho_\infty^\pi(M|s_0 = s)$ . It has been shown by Ruszczynski (2010) that this value function can be found by recursively applying the *risk-sensitive* Bellman equation:

$$V^\pi(s) = R(s, \pi(s)) + \gamma \min_{\xi \in \mathcal{B}_\rho(T(s, \pi(s), \cdot))} \sum_{s'} T(s, \pi(s), s') \cdot \xi(s') \cdot V^\pi(s'). \quad (3)$$

Likewise, the optimal risk-sensitive value,  $V^*(s) = \max_{\pi \in \Pi} \rho_\infty(M|s_0 = s)$ , is the unique solution to the risk-sensitive Bellman optimality equation:

$$V^*(s) = \max_{a \in A} \left\{ R(s, a) + \gamma \min_{\xi \in \mathcal{B}_\rho(T(s, a, \cdot))} \sum_{s'} T(s, a, s') \cdot \xi(s') \cdot V^*(s') \right\} \quad (4)$$

Thus, we can view Markov dynamic risk measures as the expected value in an MDP where the transition probabilities at each step are modified adversarially within the risk-envelope for the chosen one-step static risk measure.

## 4. One Risk to Rule Them All

In this section, we present *One Risk to Rule Them All* (1R2R), a new algorithm for risk-sensitive offline RL. Our model-based approach assumes that we can compute an approximation to the posterior distribution over MDPs, given the offline dataset. 1R2R then uses an RL algorithm to train a policy using synthetic data generated from the distribution over MDP models. To achieve risk-sensitivity, the data distribution of the model rollouts is modified according to the risk envelope of the chosen risk measure. This simple modification to standard model-based RL enables our approach to avoid distributional shift, and generate risk-sensitive behaviour.

### 4.1. Problem Formulation

For ease of exposition, we will assume that the reward function is known and therefore it is only the transition function that must be learned. Given the offline dataset,  $\mathcal{D}$ , we assume that we can approximate the posterior distribution over the MDP transition function given the dataset:  $P(T | \mathcal{D})$ . We can integrate over all possible transition functions to obtain a single transition function:

$$\bar{T}(s, a, s') = \int_T T(s, a, s') \cdot P(T | \mathcal{D}) \cdot dT. \quad (5)$$

This gives rise to a single MDP representing the distribution over plausible MDPs,  $\bar{M} = (S, A, \bar{T}, R, s_0, \gamma)$ . This is conceptually similar to the *Bayes-Adaptive* MDP (Duff, 2002; Ghavamzadeh et al., 2015), except that in the Bayes-Adaptive MDP the posterior distribution over transition functions is updated after each step of online interaction with the environment. Here, we assume that the posterior distribution is fixed given the offline dataset. To make this distinction, we refer to  $\bar{M}$  as the Bayesian MDP (BMDP). We defer the interested reader to Dorfman et al. (2021) and Ghosh et al. (2022) for work on Bayes-Adaptive offline RL.

In this work, we pose the problem of offline RL as optimising the dynamic risk in the BMDP induced by the dataset.

*Problem 1.* Given an offline dataset,  $\mathcal{D}$ , static risk measure  $\rho$ , and belief over the transition dynamics given the dataset,  $P(T | \mathcal{D})$ , find the policy with the optimal dynamic risk in the corresponding Bayesian MDP  $\bar{M}$ :

$$\pi^* = \arg \max_{\pi} \rho_\infty^\pi(\bar{M}) \quad (6)$$

### 4.2. Motivation

Equation 3 shows that dynamic risk in MDPs is equivalent to the expected value, but with the transition distribution perturbed by  $\xi(s')$  at each step. The perturbation is adversarial, so transitions to low-value successor states are made more likely, and vice-versa. Consider some low-value successor state,  $s'$ . A perturbation to increase the BMDP transition probability  $\bar{T}(s, a, s')$  can be written as:

$$\begin{aligned} \xi(s') \cdot \bar{T}(s, a, s') &= \xi(s') \cdot \int_T T(s, a, s') \cdot P(T | \mathcal{D}) \cdot dT \\ &= \int_{T \in \{T | T(s, a, s') \neq 0\}} \xi(s') \cdot T(s, a, s') \cdot P(T | \mathcal{D}) \cdot dT \end{aligned} \quad (7)$$

Thus, we can view  $\xi(s')$  as jointly perturbing the belief distribution  $P(T | \mathcal{D})$  and the corresponding transition probability  $T(s, a, s')$ , for transition functions where  $T(s, a, s') \neq 0$ , such that the overall likelihood of transitioning to low-value successor state  $s'$  is increased. This

increases the likelihood of transitioning to low-value successor states that are plausible due to either epistemic uncertainty (represented by  $P(T | \mathcal{D})$ ) or aleatoric uncertainty (represented by  $T(s, a, \cdot)$ ). Thus, the adversarial perturbation results in aversion to both sources of uncertainty.

This idea is illustrated by the example in Figure 1. The example shows a dataset drawn from a heteroskedastic transition function. Each episode consists of one step. A single reward is received, equal to the value of the successor state. We approximate  $P(T | \mathcal{D})$  using an ensemble of neural networks, and the shaded region represents the aggregated BMDP transition function  $\bar{T}(s, a, s')$ . The dashed red line indicates the Q-values computed by drawing transitions from  $\bar{T}(s, a, s')$ . For this value function, the action with the highest Q-value is  $a = 1$ , which is outside of the data distribution. The solid red line indicates the *risk-sensitive* value function for the risk measure  $\text{CVaR}_{0.1}$  (i.e.  $\alpha = 0.1$ ). This is computed by drawing transitions from a uniform distribution over the worst 10% of transitions from  $\bar{T}(s, a, s')$ . We can see that the risk-sensitive value function penalises straying far from the dataset, where epistemic uncertainty is high. The action in the dataset with highest expected value is  $a = 0.4$ . However, the action  $a = -0.35$  has a higher risk-sensitive value than  $a = 0.4$ , due to the latter having high-variance transitions (i.e. high aleatoric uncertainty). Thus, we see that choosing actions according to the risk-sensitive value function penalises actions with high uncertainty due to either epistemic or aleatoric uncertainty.

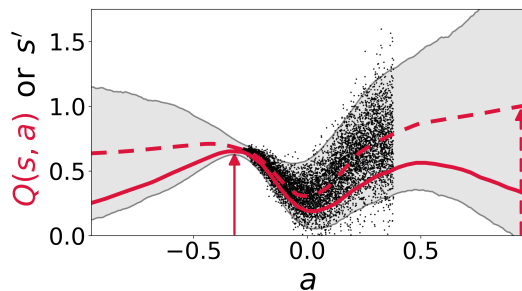


Figure 1: MDP where there is a single transition to a successor state  $s'$ , where a reward  $R(s') = s'$  is received. The dataset is illustrated by the black dots. The shaded region indicates  $\pm 2$  S.D. of successor states drawn from an approximation of  $\bar{T}(s, a, \cdot)$ . This approximation is a uniform distribution over an ensemble of probabilistic neural networks (Chua et al., 2018). The dashed red line indicates the Q-values from running MBPO (Janner et al., 2019). The solid red line indicates the risk-sensitive value function computed by reweighting the transitions generated by the ensemble according to  $\text{CVaR}_{0.1}$ . Arrows indicate optimal actions according to each Q-function.

### 4.3. Approach

Our approach is based on Model-Based Policy Optimisation (Janner et al., 2019). We perform truncated rollouts within the learnt model  $\hat{T}$ , and use this synthetic data to optimise a policy using an off-policy RL algorithm. Our algorithm is inspired by the model-free online RL method for aleatoric risk introduced by Tamar et al. (2015a), but we have adapted it to the model-based offline RL setting.

The key idea of our approach is that to achieve risk-sensitivity, we modify the distribution of trajectories sampled in the model. Following Equation 3, we first compute the adversarial perturbation to the transition distribution:

$$\xi^* = \arg \min_{\xi \in \mathcal{B}_\rho(\bar{T}(s, a, \cdot))} \sum_{s'} \bar{T}(s, a, s') \cdot \xi(s') \cdot V^\pi(s'), \quad (8)$$

where  $V^\pi$  is estimated by the standard off-policy RL algorithm. When generating synthetic rollouts from the model, for each state-action pair  $(s, a)$  we sample successor states from the perturbed distribution  $\xi^* \cdot \bar{T}$ :

$$s' \sim \xi^*(s') \cdot \bar{T}(s, a, s') \quad \forall s' \quad (9)$$

The transition data generated from this modified distribution is added to the synthetic dataset,  $\hat{\mathcal{D}}$ . This approach modifies the sampling distribution over successor states according to the risk-sensitive Bellman equation in Equation 3. Therefore, the value function learnt by the actor-critic RL algorithm under this modified sampling distribution is equal to the risk-sensitive value function. The policy is then optimised to maximise the risk-sensitive value function.

For the continuous problems we address, it is difficult to compute the adversarially modified transition distribution by solving the optimisation problem in Equation 8 exactly. Therefore, we use sample average approximation (SAA) (Shapiro et al., 2021a) to approximate the solution to Equation 8. Specifically, we approximate  $\bar{T}(s, a, \cdot)$  as a uniform distribution over  $m$  states drawn from  $\bar{T}(s, a, \cdot)$ . Then, we compute the optimal adversarial perturbation to this uniform distribution over successor states. Under standard regularity assumptions, the solution to the SAA converges to the exact solution as  $m \rightarrow \infty$  (Shapiro et al., 2021a).

**Algorithm** Our approach is summarised in Algorithm 1. At each iteration, we generate  $N_{\text{rollout}}$  truncated synthetic rollouts which are branched from an initial state sampled from the dataset (Lines 3-5). For a given  $(s, a)$  pair we sample a set  $\Psi$  of  $m$  candidate successor states from  $\bar{T}$  (Line 7). We then approximate the original transition distribution by  $\hat{T}$ , a uniform distribution over  $\Psi$ , in Line 8. Under this approximation, it is straightforward to compute the worst-case perturbed transition distribution for the given risk measure in Line 9. Details of how this is computed for CVaR and the Wang risk are in Appendix A. The final successor state  $s'$  is

---

**Algorithm 1** 1R2R

---

**Require:** Offline dataset,  $\mathcal{D}$ ; Static risk measure,  $\rho$ ;

- 1: Compute belief distribution over transition models,  $P(T | \mathcal{D})$ ;
- 2: **for** iter = 1, ...,  $N_{\text{iter}}$  :
- 3:     **for** rollout = 1, ...,  $N_{\text{rollout}}$ , generate synthetic rollouts:
- 4:         Sample initial state,  $s \in \mathcal{D}$ .
- 5:         **for** step = 1, ...,  $k$  :
- 6:             Sample action  $a$  according to current policy  $\pi(s)$ .
- 7:             Sample  $m$  successor states,  $\Psi = \{s'_i\}_{i=1}^m$  from  $\bar{T}(s, a, \cdot)$ .
- 8:             Consider  $\hat{T}$ , a discrete approximation to  $\bar{T}$ :
 
$$\hat{T}(s, a, s') \approx \bar{T}(s, a, s') = \frac{1}{m}, \forall s' \in \Psi$$
- 9:             Compute adversarial perturbation to  $\hat{T}$ :
 
$$\hat{\xi}^* = \arg \min_{\xi \in \mathcal{B}_\rho(\hat{T}(s, a, \cdot))} \sum_{s' \in \Psi} \hat{T}(s, a, s') \cdot \xi(s') \cdot V^\pi(s')$$
- 10:             Sample from adversarially modified distribution:
 
$$s' \sim \hat{\xi}^* \cdot \hat{T}(s, a, \cdot)$$
- 11:             Add  $(s, a, R(s, a), s')$  to the synthetic dataset,  $\hat{\mathcal{D}}$ .
- 12:              $s \leftarrow s'$
- 13:     Agent update: Update  $\pi$  and  $V^\pi$  with an actor-critic algorithm, using samples from  $\mathcal{D} \cup \hat{\mathcal{D}}$ .

---

sampled from the perturbed distribution in Line 10 and it is the transition to this final successor state that is added to the synthetic dataset.

After the synthetic rollouts have been generated, the policy and value function are updated using an off-policy actor-critic algorithm by sampling data from both the synthetic dataset and the real dataset (Line 13). We found that additionally utilising the real data improves performance.

#### 4.4. Implementation Details

As an approximation for  $P(T | \mathcal{D})$ , we use a uniform distribution over an ensemble of neural networks. This follows from a number of previous works that use ensembles to approximate a distribution over models (Guo et al., 2022; Rajeswaran et al., 2017; Yu et al., 2020). Like previous works, each model in the ensemble,  $T_i$ , outputs a Gaussian distribution over successor states as well as rewards:  $T_i(s', r | s, a) = \mathcal{N}(\mu_i(s, a), \Sigma_i(s, a))$ . We used soft-actor critic (SAC) (Haarnoja et al., 2018) as the off-policy actor-critic algorithm in Line 13. For policy improvement, we used the standard policy gradient that is utilised by SAC. We found that this worked well in practice and meant that our approach requires minimal modifications to existing RL algorithms. Research on specialised policy gradients for risk-sensitive objectives can be found in Tamar et al. (2015a); Chow et al. (2017).

## 5. Experiments

In our experiments, we seek to: a) verify that 1R2R generates performant policies in deterministic environments by avoiding distributional shift, b) investigate whether 1R2R generates risk-sensitive behaviour on stochastic domains, and c) compare the performance of 1R2R against existing baselines on both stochastic and deterministic environments. The code for our experiments will be made publicly available. Please contact the lead author for details.

To examine each of these questions, we evaluate our approach on the following domains. More information about the domains can be found in Appendix D.2.

**D4RL MuJoCo** (Fu et al., 2020) There are three different environments representing different robots (*HalfCheetah*, *Hopper*, *Walker2D*), each with 4 datasets (*Random*, *Medium*, *Medium-Replay*, *Medium-Expert*). *Random* contains transitions collected by a random policy. *Medium* contains transitions collected by an early-stopped SAC policy. *Medium-Replay* consists of the replay buffer generated while training the *Medium* policy. The *Medium-Expert* dataset contains a mixture of sub-optimal and expert data.

**Currency Exchange** We adapt the Optimal Liquidation problem (Almgren & Chriss, 2001; Bao & Liu, 2019) to offline RL. The agent aims to convert 100 units of currency A to currency B, subject to a stochastically changing exchange rate, before a deadline. The dataset consists of experience from a random policy.

**HIV Treatment** We adapt this online RL domain (Keramati et al., 2020; Ernst et al., 2006) to the offline setting. The 6-dimensional continuous state vector represents the concentrations of various cells and viruses. The actions correspond to the dosages of two drugs. Transitions are stochastic due to the efficacy of each drug varying stochastically at each step. The reward is determined by the health outcomes for the patient, and penalises side-effects due to the quantity of drugs prescribed. The dataset is constructed in the same way as the D4RL *Medium-Replay* datasets.

**Stochastic MuJoCo** We modify the D4RL benchmarks by adding stochastic perturbation forces to the environment. We opt to focus on the Hopper and Walker2D domains as there is a risk that any episode may terminate early due to the robot falling over. We vary the magnitude of the perturbations between two different levels (*Moderate-Noise*, *High-Noise*). For each domain and noise level we construct *Medium*, *Medium-Replay*, and *Medium-Expert* datasets in the same fashion as D4RL.

**Baselines** We compare 1R2R against offline RL algorithms designed for risk-sensitive optimisation (ORAAC (Urpí et al., 2021) and CODAC (Ma et al., 2021)) in addition to performant risk-neutral model-

based (RAMBO (Rigter et al., 2022b)) and model-free (IQL (Kostrikov et al., 2022), TD3+BC (Fujimoto & Gu, 2021), and CQL (Kumar et al., 2020)) algorithms. For the D4RL benchmarks, we provide results for the -v2 datasets.

**Hyperparameters** For risk-sensitive algorithms ORAAC and CODAC, we set the optimisation objective to the desired objective for each domain. For all baselines, we tune hyperparameters to obtain the best online performance for the desired objective on each dataset (see Appendix D.5). Likewise, we tune the hyperparameters for 1R2R (the rollout length and risk measure parameter) to achieve the best online performance as described in Appendix C.4.

**Versions of 1R2R** We test two versions 1R2R which each utilise different risk measures to re-weight the transition distribution to successor states:  $1R2R_{CVaR}$  and  $1R2R_{Wang}$ . These risk measures are defined in Section 3. We chose CVaR because it is commonly used and easy to interpret. However, CVaR disregards the best possible outcomes, and this can lead to an unnecessary loss in performance (Rigter et al., 2022a). Therefore, we also trial the Wang risk measure which makes use of the entire distribution over outcomes. Furthermore, we present additional results that we reference as the ‘‘Ablation’’. To generate these results we run 1R2R without modifying the transition distribution of the rollouts, i.e. without risk-aversion.

**Normalisation** Following Fu et al. (2020), the results in Tables 1, 2, and 3 are normalised so that 0 represents the average performance of a randomly initialised policy, and 100 represents the average performance of an expert policy. The values used for the normalisation are in Appendix D.2.

### 5.1. Results

**D4RL MuJoCo** For these domains, the objective is to optimise the expected performance. Thus, to generate the results in Table 1 we configure all algorithms to obtain the best expected performance. The results in Table 1 show that similar results are obtained by both  $1R2R_{CVaR}$  and  $1R2R_{Wang}$ . The performance of both configurations of 1R1R is competitive with the risk-neutral baselines on these deterministic domains. 1R2R outperforms ORAAC and CODAC, the two existing offline RL algorithms that are able to take risk into consideration. The ablation shows that when risk-sensitivity is removed from 1R2R, for many domains the training diverges or performance degrades. This verifies that the consideration of risk in our approach is crucial for ensuring that the policy avoids distributional shift.

For some datasets (especially those for HalfCheetah), the ablation obtains similar performance to 1R2R. This shows that for some problems, standard model-based RL can be successful in the offline setting.

**Currency Exchange** We use this toy example to qualitatively examine the trade-off between risk and expected performance achieved by 1R2R. In Figure 2, we observe that the risk-neutral algorithm, RAMBO, obtains the best performance in expectation. However, the return distribution for RAMBO includes a considerable tail of poor outcomes as evidenced by the static  $CVaR_{0.1}$  performance for RAMBO. For 1R2R, we observe that as we use a more risk-averse dynamic risk measure, the resulting behaviour becomes more risk-averse. For more risk-averse parameter settings, the number of poor outcomes in the tail of the return distribution is reduced, at the expense of worse performance in expectation. These results verify that by adjusting the dynamic risk measure, we are able to obtain different levels of risk-sensitivity towards aleatoric uncertainty with 1R2R.

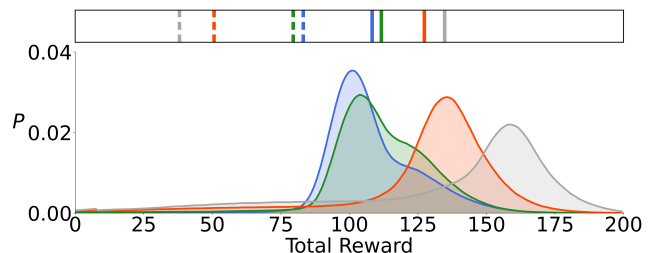


Figure 2: Unnormalized return distributions for the Currency Exchange domain, aggregated over 10 seeds. Results are generated by 1R2R with the following risk measures for the dynamic risk:  $CVaR_{0.5}$  (blue);  $CVaR_{0.7}$  (green);  $CVaR_{0.9}$  (red). The return distribution for risk-neutral RAMBO is grey. Solid vertical bars indicate average return, dashed vertical bars indicate the mean of the worst 10% of returns (i.e. static  $CVaR_{0.1}$ ).

**HIV Treatment** As this is a healthcare setting, we assume that the desired behaviour is to be highly risk-averse. Therefore, we assume that the objective is to optimise static  $CVaR_{0.02}$ , and configure all algorithms to obtain the best performance for this objective. Results for this objective, as well as the expected performance for each algorithm are in Table 2. We observe that 1R2R obtains the best performance for the static  $CVaR_{0.02}$  objective. RAMBO obtains similar, yet slightly worse performance. The return distributions for each algorithm in Appendix B.2 show that the policies obtained by 1R2R generate qualitatively different behaviour than RAMBO. This suggests that 1R2R generates a different policy from RAMBO, that is more tailored towards risk-aversion. TD3+BC obtains similar performance to 1R2R for the expected value objective, but performs much worse for static  $CVaR_{0.02}$ . This shows that strong expected performance is not sufficient to ensure good performance in the worst outcomes. ORAAC and CODAC, the risk sensitive-algorithms which are configured to optimise static  $CVaR_{0.02}$ , both perform poorly. One explanation for

Table 1: Normalised expected value results for the D4RL MuJoCo-v2 benchmark. We report the average return during the last 10 iterations of training averaged over 5 seeds. Highlighted numbers indicate results within 10% of the best score.  $\pm$  indicates the S.D. over seeds. “div.” indicates that the value function diverged for at least one run.

		1R2R <sub>CVaR</sub>	1R2R <sub>Wang</sub>	Ablation	ORAAC	CODAC	RAMBO	CQL	IQL	TD3+BC
Random	HalfCheetah	36.9 $\pm$ 6.4	35.5 $\pm$ 1.7	38.6 $\pm$ 1.9	22.4 $\pm$ 1.7	31.0 $\pm$ 2.0	40.0	19.6	-	11.0
	Hopper	30.9 $\pm$ 2.3	31.8 $\pm$ 0.2	div.	10.9 $\pm$ 13.3	9.2 $\pm$ 0.7	21.6	6.7	-	8.5
	Walker2D	7.6 $\pm$ 12.2	8.1 $\pm$ 11.0	div.	2.4 $\pm$ 3.5	12.8 $\pm$ 8.9	11.5	2.4	-	1.6
Medium	HalfCheetah	74.5 $\pm$ 2.1	75.5 $\pm$ 1.2	76.9 $\pm$ 1.2	38.5 $\pm$ 4.8	62.8 $\pm$ 0.9	77.6	49.0	47.4	48.3
	Hopper	80.2 $\pm$ 15.8	64.6 $\pm$ 25.1	64.4 $\pm$ 18.5	29.6 $\pm$ 10.3	63.9 $\pm$ 1.7	92.8	66.6	66.3	59.3
	Walker2D	63.9 $\pm$ 31.8	83.4 $\pm$ 4.8	85.3 $\pm$ 0.0	45.5 $\pm$ 14.9	84.0 $\pm$ 4.0	86.9	83.8	78.3	83.7
Medium Replay	HalfCheetah	65.7 $\pm$ 2.3	65.6 $\pm$ 1.3	65.9 $\pm$ 3.4	39.3 $\pm$ 1.7	53.4 $\pm$ 1.9	68.9	47.1	44.2	44.6
	Hopper	92.9 $\pm$ 10.7	93.2 $\pm$ 8.7	55.3 $\pm$ 14.4	22.6 $\pm$ 12.1	68.8 $\pm$ 28.2	96.6	97.0	94.7	60.9
	Walker2D	92.2 $\pm$ 2.3	88.4 $\pm$ 5.0	92.7 $\pm$ 3.6	11.1 $\pm$ 5.6	73.9 $\pm$ 31.7	85.0	88.2	73.9	81.8
Medium Expert	HalfCheetah	96.0 $\pm$ 6.0	94.5 $\pm$ 1.9	87.8 $\pm$ 6.3	24.4 $\pm$ 7.6	76.7 $\pm$ 4.9	93.7	90.8	86.7	90.7
	Hopper	81.6 $\pm$ 22.9	89.6 $\pm$ 17.8	88.6 $\pm$ 13.4	4.1 $\pm$ 2.8	87.6 $\pm$ 6.4	83.3	106.8	91.5	98.0
	Walker2D	90.9 $\pm$ 5.9	78.1 $\pm$ 7.9	div.	42.8 $\pm$ 9.2	112.0 $\pm$ 2.3	68.3	109.4	109.6	110.1

the poor performance of these algorithms is that it is difficult to accurately estimate the tail of the return distribution from a limited dataset. Estimating the tail of the distribution is necessary directly optimise static CVaR<sub>0.02</sub> using distributional RL. In contrast, the dynamic risk approach that we propose recursively introduces risk-aversion at each step to generate behaviour that is highly risk-averse overall. Therefore, our approach does not need to estimate the extreme tails of any distribution.

For the static CVaR<sub>0.02</sub> objective, 1R2R and RAMBO both outperform a SAC agent that has been trained online. This is despite only having access to considerably less training data that was generated by a sub-optimal SAC agent. This verifies that it is possible for offline RL algorithms to recombine existing data to obtain better risk-sensitive performance.

Table 2: Normalized performance on the HIV Treatment domain. The results are generated from 500 evaluation episodes at each of the last 10 iterations of training, and averaged over 10 seeds. Highlighted numbers indicate results within 10% of the best score.  $\pm$  indicates S.D. over seeds.

Algorithm	Static CVaR <sub>0.02</sub>	Expected Value
1R2R <sub>CVaR</sub>	43.7 $\pm$ 1.5	73.5 $\pm$ 1.9
1R2R <sub>Wang</sub>	42.3 $\pm$ 3.9	68.9 $\pm$ 7.5
Ablation	33.9 $\pm$ 17.9	56.7 $\pm$ 30.1
ORAAC	0.1 $\pm$ 0.1	3.7 $\pm$ 6.7
CODAC	9.1 $\pm$ 1.3	58.7 $\pm$ 1.5
RAMBO	42.0 $\pm$ 1.5	73.2 $\pm$ 1.2
CQL	12.5 $\pm$ 2.3	63.5 $\pm$ 1.8
IQL	0.0 $\pm$ 0.0	27.1 $\pm$ 4.9
TD3+BC	19.1 $\pm$ 5.5	70.2 $\pm$ 1.2
SAC (Online)	38.4 $\pm$ 9.6	100.0 $\pm$ 18.2

**Stochastic MuJoCo** Following previous works (Urpí et al., 2021; Ma et al., 2021), we assume that the objec-

tive for these domains is to optimise static CVaR<sub>0.1</sub>. The performance of each algorithm for static CVaR<sub>0.1</sub> is in Table 3, and the performance for expected value is in Table 4 in the appendix. We observe that 1R2R<sub>CVaR</sub> performs the best for static CVaR<sub>0.1</sub> in the *Medium* and *Medium-Replay* datasets. For these benchmarks, 1R2R<sub>Wang</sub> performs worse than 1R2R<sub>CVaR</sub>. A possible explanation is that because the Wang risk measure makes use of the entire distribution over outcomes, 1R2R<sub>Wang</sub> trains the policy on some over-optimistic data. On the other hand, 1R2R<sub>CVaR</sub> disregards the most optimistic outcomes, resulting in more robust performance. For the ablation, either training diverges or the performance degrades relative to 1R2R<sub>CVaR</sub> for most datasets.

1R2R<sub>CVaR</sub> considerably outperforms ORAAC and CODAC, the two prior algorithms for risk-sensitive offline RL. Interestingly, while IQL performs well for the deterministic benchmarks, it performs very poorly for the *Medium-Replay* stochastic benchmarks. This suggests that we should not rely on deterministic domains to benchmark algorithms. CQL and TD3+BC both obtain fairly strong performance. They easily outperform 1R2R<sub>CVaR</sub> on the *Medium-Expert* datasets, where 1R2R performs poorly. These results, and the results for CODAC and ORAAC, indicate that there is still progress to be made towards developing better risk-sensitive offline RL algorithms.

Finally, the expected value results in Table 4 show that 1R2R<sub>CVaR</sub> performs slightly less well for expected performance than static CVaR<sub>0.1</sub>, compared to the baselines. However, there is a strong correlation between the results for expected value and the results for static CVaR<sub>0.1</sub>. This indicates that for these domains, there is only a modest tradeoff between risk and expected performance.

Table 3: Normalised static CVaR<sub>0.1</sub> results for Stochastic MuJoCo. We report static CVaR<sub>0.1</sub> evaluated over the last 10 iterations of training, and averaged over 5 seeds. Highlighted numbers indicate results within 10% of the best score. ± indicates the S.D. over seeds. “div.” indicates that the value function diverged for at least one run.

		1R2R <sub>CVaR</sub>	1R2R <sub>Wang</sub>	Ablation	ORAAC	CODAC	RAMBO	CQL	IQL	TD3+BC
Medium	Hopper (Mod)	36.9 ± 5.1	37.3 ± 1.9	35.7 ± 2.9	10.2 ± 3.9	33.6 ± 0.1	37.8 ± 8.3	33.5 ± 0.1	33.0 ± 1.4	33.4 ± 0.1
	Walker2D (Mod)	29.9 ± 8.7	28.3 ± 4.2	7.7 ± 11.6	17.7 ± 4.6	26.8 ± 0.8	8.0 ± 0.5	32.0 ± 1.7	22.7 ± 2.3	22.9 ± 11.5
	Hopper (High)	38.6 ± 3.0	42.0 ± 1.2	40.2 ± 1.2	18.5 ± 10.0	36.8 ± 0.3	36.5 ± 7.3	38.7 ± 0.8	35.8 ± 0.9	37.4 ± 0.5
	Walker2D (High)	19.2 ± 12.6	19.5 ± 5.2	div.	6.3 ± 7.4	32.2 ± 3.6	19.7 ± 0.7	43.1 ± 2.7	16.7 ± 3.5	48.2 ± 3.4
Medium Replay	Hopper (Mod)	43.9 ± 11.7	37.1 ± 7.6	33.6 ± 2.8	7.4 ± 1.3	32.1 ± 4.7	35.1 ± 5.7	34.1 ± 2.2	-0.6 ± 0.0	24.2 ± 2.3
	Walker2D (Mod)	30.1 ± 7.2	28.0 ± 7.1	29.7 ± 2.2	4.7 ± 2.5	23.3 ± 10.4	30.9 ± 5.7	25.4 ± 1.9	1.4 ± 0.6	28.8 ± 1.0
	Hopper (High)	51.4 ± 8.1	46.1 ± 7.9	30.5 ± 10.9	14.7 ± 15.2	38.9 ± 0.8	36.4 ± 8.6	50.9 ± 2.8	7.3 ± 5.8	35.5 ± 2.0
	Walker2D (High)	46.0 ± 10.1	28.8 ± 5.2	30.9 ± 14.3	1.1 ± 0.8	43.1 ± 14.4	42.2 ± 10.4	15.6 ± 6.1	-1.2 ± 0.3	29.9 ± 6.8
Medium Expert	Hopper (Mod)	65.4 ± 31.7	45.7 ± 35.7	32.6 ± 26.3	14.9 ± 9.6	44.1 ± 10.9	32.0 ± 12.6	60.6 ± 11.7	75.0 ± 29.7	54.2 ± 3.3
	Walker2D (Mod)	34.8 ± 6.5	38.5 ± 8.9	div.	14.7 ± 3.6	28.1 ± 12.5	29.9 ± 14.2	72.3 ± 9.0	24.5 ± 1.2	68.4 ± 2.7
	Hopper (High)	35.5 ± 5.7	39.3 ± 4.6	30.5 ± 7.4	9.1 ± 9.4	47.1 ± 1.7	38.5 ± 2.1	47.1 ± 2.1	32.6 ± 4.3	51.0 ± 1.3
	Walker2D (High)	10.8 ± 4.3	11.7 ± 5.2	div.	4.2 ± 6.2	26.7 ± 16.5	1.9 ± 1.4	55.5 ± 5.5	28.0 ± 8.8	60.2 ± 8.9

## 6. Discussion and Conclusion

**Static vs Dynamic Risk** We chose to base our approach on dynamic risk, which evaluates risk recursively at each step, rather than static risk which evaluates risk across episodes. The dynamic risk perspective is arguably more suitable for avoiding distributional shift, as it enforces aversion to uncertainty at each time step, thus preventing the policy from leaving the data-distribution at any step. It is also more amenable to our model-based approach, where we modify the transition distribution of synthetic data at each step to achieve risk-aversion. Applying this same approach to the static risk setting would likely require modifying the distribution over entire trajectories (Chow et al., 2017; Tamar et al., 2015b). However, sampling full length trajectories is not desirable in model-based methods due to compounding modelling error (Janner et al., 2019). The disadvantage of dynamic risk is that it is difficult to choose the risk measure to apply and it can lead to overly conservative behaviour (Gagne & Dayan, 2021).

**Uncertainty Modelling** To model the uncertainty over the transition model, we use a uniform distribution over a neural network ensemble following from previous works (Guo et al., 2022; Rajeswaran et al., 2017; Yu et al., 2020). However, this may result in inaccurate uncertainty estimation (Yu et al., 2021). Furthermore, the transition distribution for each model is Gaussian. This means that our implementation is not suitable for domains with multimodal dynamics, such as those proposed by Urfi et al. (2021). To improve our approach, an obvious next step is to utilise better models of stochasticity that can handle general multimodal distributions (Hafner et al., 2021). Our approach would also benefit from improved techniques for uncertainty estimation (Gawlikowski et al., 2021). A straightforward first step would be to test our approach with a much larger ensemble, which has been found to obtain strong perfor-

mance in other works (Guo et al., 2022; Lu et al., 2022).

**Epistemic vs Aleatoric Uncertainty** Our approach is agnostic to the source of uncertainty. This is motivated by the intuition that poor outcomes should be avoided due to either source of uncertainty. There are two modifications that we leave to future work. The first is to marginalise out the aleatoric uncertainty and consider risk-aversion only to epistemic uncertainty (Sharma et al., 2019). The second is to use composite risk measures (Eriksson et al., 2022), which enable the aversion to each source of risk to be adjusted independently. The latter approach might be useful for achieving strong performance even if the estimation of each source of uncertainty is poorly calibrated.

**Conclusion** We have proposed 1R2R, a new model-based algorithm for risk-sensitive offline RL. The key idea behind our approach is that optimising for risk-aversion can be used to solve the issue of distributional shift, in addition to achieving aversion to aleatoric risk. In this work, we developed an algorithm that is agnostic to the source of uncertainty. As discussed, a key direction for future work is to investigate methods that apply different levels of risk-aversion to each source of uncertainty (Eriksson et al., 2022).

## References

- Agarwal, R., Schuurmans, D., and Norouzi, M. An optimistic perspective on offline reinforcement learning. In *International Conference on Machine Learning*, pp. 104–114. PMLR, 2020.
- Almgren, R. and Chriss, N. Optimal execution of portfolio transactions. *Journal of Risk*, 3:5–40, 2001.
- An, G., Moon, S., Kim, J.-H., and Song, H. O. Uncertainty-based offline reinforcement learning with diversified Q-ensemble. *Advances in Neural Information Processing Systems*, 34:7436–7447, 2021.
- Argenson, A. and Dulac-Arnold, G. Model-based offline planning. In *International Conference on Learning Representations*, 2021.
- Artzner, P., Delbaen, F., Eber, J.-M., and Heath, D. Coherent measures of risk. *Mathematical finance*, 9(3):203–228, 1999.
- Ball, P. J., Lu, C., Parker-Holder, J., and Roberts, S. Augmented world models facilitate zero-shot dynamics generalization from a single offline environment. In *International Conference on Machine Learning*, pp. 619–629. PMLR, 2021.
- Bao, W. and Liu, X.-y. Multi-agent deep reinforcement learning for liquidation strategy analysis. *arXiv preprint arXiv:1906.11046*, 2019.
- Bellemare, M. G., Dabney, W., and Munos, R. A distributional perspective on reinforcement learning. In *International Conference on Machine Learning*, pp. 449–458. PMLR, 2017.
- Boda, K. and Filar, J. A. Time consistent dynamic risk measures. *Mathematical Methods of Operations Research*, 63(1):169–186, 2006.
- Cheng, C.-A., Xie, T., Jiang, N., and Agarwal, A. Adversarially trained actor critic for offline reinforcement learning. 2022.
- Chow, Y., Tamar, A., Mannor, S., and Pavone, M. Risk-sensitive and robust decision-making: a CVaR optimization approach. *Advances in Neural Information Processing Systems*, 28, 2015.
- Chow, Y., Ghavamzadeh, M., Janson, L., and Pavone, M. Risk-constrained reinforcement learning with percentile risk criteria. *The Journal of Machine Learning Research*, 18(1):6070–6120, 2017.
- Chua, K., Calandra, R., McAllister, R., and Levine, S. Deep reinforcement learning in a handful of trials using probabilistic dynamics models. *Advances in Neural Information Processing Systems*, 31, 2018.
- Clements, W. R., Van Delft, B., Robaglia, B.-M., Slaoui, R. B., and Toth, S. Estimating risk and uncertainty in deep reinforcement learning. *ICML Workshop on Uncertainty and Robustness in Deep Learning*, 2020.
- Dabney, W., Ostrovski, G., Silver, D., and Munos, R. Implicit quantile networks for distributional reinforcement learning. In *International Conference on Machine Learning*, pp. 1096–1105. PMLR, 2018.
- Depeweg, S., Hernandez-Lobato, J.-M., Doshi-Velez, F., and Udluft, S. Decomposition of uncertainty in Bayesian deep learning for efficient and risk-sensitive learning. In *International Conference on Machine Learning*, pp. 1184–1193. PMLR, 2018.
- Dorfman, R., Shenfeld, I., and Tamar, A. Offline meta reinforcement learning – identifiability challenges and effective data collection strategies. In *Advances in Neural Information Processing Systems*, volume 34, 2021.
- Duff, M. O. *Optimal Learning: Computational procedures for Bayes-adaptive Markov decision processes*. University of Massachusetts Amherst, 2002.
- Eriksson, H. and Dimitrakakis, C. Epistemic risk-sensitive reinforcement learning. *European Symposium on Artificial Neural Networks, Computational Intelligence and Machine Learning*, 2020.
- Eriksson, H., Basu, D., Alibeigi, M., and Dimitrakakis, C. Sentinel: taming uncertainty with ensemble based distributional reinforcement learning. In *Uncertainty in Artificial Intelligence*, pp. 631–640. PMLR, 2022.
- Ernst, D., Stan, G.-B., Goncalves, J., and Wehenkel, L. Clinical data based optimal STI strategies for HIV: a reinforcement learning approach. In *Proceedings of the 45th IEEE Conference on Decision and Control*, pp. 667–672. IEEE, 2006.
- Fu, J., Kumar, A., Nachum, O., Tucker, G., and Levine, S. D4RL: Datasets for deep data-driven reinforcement learning. *arXiv preprint arXiv:2004.07219*, 2020.
- Fujimoto, S. and Gu, S. S. A minimalist approach to offline reinforcement learning. *Advances in Neural Information Processing Systems*, 34, 2021.
- Fujimoto, S., Meger, D., and Precup, D. Off-policy deep reinforcement learning without exploration. In *International Conference on Machine Learning*, pp. 2052–2062. PMLR, 2019.
- Gagne, C. and Dayan, P. Two steps to risk sensitivity. *Advances in Neural Information Processing Systems*, 34: 22209–22220, 2021.

- Garcia, J. and Fernández, F. A comprehensive survey on safe reinforcement learning. *Journal of Machine Learning Research*, 16(1):1437–1480, 2015.
- Gawlikowski, J., Tassi, C. R. N., Ali, M., Lee, J., Humt, M., Feng, J., Kruspe, A., Triebel, R., Jung, P., Roscher, R., et al. A survey of uncertainty in deep neural networks. *arXiv preprint arXiv:2107.03342*, 2021.
- Geramifard, A., Dann, C., Klein, R. H., Dabney, W., and How, J. P. RLPy: a value-function-based reinforcement learning framework for education and research. *Journal of Machine Learning Research*, 16(1):1573–1578, 2015.
- Ghavamzadeh, M., Mannor, S., Pineau, J., Tamar, A., et al. Bayesian reinforcement learning: A survey. *Foundations and Trends® in Machine Learning*, 8(5-6):359–483, 2015.
- Ghosh, D., Ajay, A., Agrawal, P., and Levine, S. Offline RL policies should be trained to be adaptive. In *International Conference on Machine Learning*, pp. 7513–7530. PMLR, 2022.
- Guo, K., Shao, Y., and Geng, Y. Model-based offline reinforcement learning with pessimism-modulated dynamics belief. *Advances in Neural Information Processing Systems*, 2022.
- Haarnoja, T., Zhou, A., Abbeel, P., and Levine, S. Soft actor-critic: Off-policy maximum entropy deep reinforcement learning with a stochastic actor. In *International Conference on Machine Learning*, pp. 1861–1870. PMLR, 2018.
- Hafner, D., Lillicrap, T., Norouzi, M., and Ba, J. Mastering atari with discrete world models. *ICLR*, 2021.
- Janner, M., Fu, J., Zhang, M., and Levine, S. When to trust your model: Model-based policy optimization. *Advances in Neural Information Processing Systems*, 32, 2019.
- Jaques, N., Ghandeharioun, A., Shen, J. H., Ferguson, C., Lapedriza, A., Jones, N., Gu, S., and Picard, R. Way off-policy batch deep reinforcement learning of implicit human preferences in dialog. *arXiv preprint arXiv:1907.00456*, 2019.
- Keramati, R., Dann, C., Tamkin, A., and Brunskill, E. Being optimistic to be conservative: Quickly learning a cvar policy. In *Proceedings of the AAAI Conference on Artificial Intelligence*, volume 34, pp. 4436–4443, 2020.
- Kidambi, R., Rajeswaran, A., Netrapalli, P., and Joachims, T. MOREL: Model-based offline reinforcement learning. *Advances in Neural Information Processing Systems*, 33: 21810–21823, 2020.
- Kingma, D. P. and Ba, J. Adam: A method for stochastic optimization. *International Conference on Learning Representations*, 2015.
- Kostrikov, I., Fergus, R., Tompson, J., and Nachum, O. Offline reinforcement learning with Fisher divergence critic regularization. In *International Conference on Machine Learning*, pp. 5774–5783. PMLR, 2021.
- Kostrikov, I., Nair, A., and Levine, S. Offline reinforcement learning with implicit Q-learning. In *International Conference on Learning Representations*, 2022.
- Kumar, A., Fu, J., Soh, M., Tucker, G., and Levine, S. Stabilizing off-policy Q-learning via bootstrapping error reduction. *Advances in Neural Information Processing Systems*, 32, 2019.
- Kumar, A., Zhou, A., Tucker, G., and Levine, S. Conservative Q-learning for offline reinforcement learning. *Advances in Neural Information Processing Systems*, 33: 1179–1191, 2020.
- Kurutach, T., Clavera, I., Duan, Y., Tamar, A., and Abbeel, P. Model-ensemble trust-region policy optimization. In *International Conference on Learning Representations*, 2018.
- Levine, S., Kumar, A., Tucker, G., and Fu, J. Offline reinforcement learning: Tutorial, review, and perspectives on open problems. *arXiv preprint arXiv:2005.01643*, 2020.
- Liu, Y., Swaminathan, A., Agarwal, A., and Brunskill, E. Off-policy policy gradient with state distribution correction. *International Conference on Machine Learning RL4RealLife Workshop*, 2019.
- Lu, C., Ball, P., Parker-Holder, J., Osborne, M., and Roberts, S. J. Revisiting design choices in offline model based reinforcement learning. In *International Conference on Learning Representations*, 2022.
- Ma, X., Xia, L., Zhou, Z., Yang, J., and Zhao, Q. DSAC: Distributional soft actor critic for risk-sensitive reinforcement learning. *arXiv preprint arXiv:2004.14547*, 2020.
- Ma, Y., Jayaraman, D., and Bastani, O. Conservative offline distributional reinforcement learning. *Advances in Neural Information Processing Systems*, 34:19235–19247, 2021.
- Majumdar, A. and Pavone, M. How should a robot assess risk? towards an axiomatic theory of risk in robotics. In *Robotics Research*, pp. 75–84. Springer, 2020.
- Maller, R. A., Müller, G., and Szimayer, A. Ornstein-uhlenbeck processes and extensions. *Handbook of financial time series*, pp. 421–437, 2009.

- Matsushima, T., Furuta, H., Matsuo, Y., Nachum, O., and Gu, S. Deployment-efficient reinforcement learning via model-based offline optimization. In *International Conference on Learning Representations*, 2021.
- Morimura, T., Sugiyama, M., Kashima, H., Hachiya, H., and Tanaka, T. Parametric return density estimation for reinforcement learning. *Conference on Uncertainty in Artificial Intelligence*, 2010.
- Nachum, O., Dai, B., Kostrikov, I., Chow, Y., Li, L., and Schuurmans, D. AlgaeDICE: Policy gradient from arbitrary experience. *arXiv preprint arXiv:1912.02074*, 2019.
- Nie, X., Brunskill, E., and Wager, S. Learning when-to-treat policies. *Journal of the American Statistical Association*, 116(533):392–409, 2021.
- Popko, W., Wächter, M., and Thomas, P. Verification of continuous time random walk wind model. In *The 26th International Ocean and Polar Engineering Conference*. OnePetro, 2016.
- Puterman, M. L. *Markov decision processes: Discrete stochastic dynamic programming*. John Wiley & Sons, 2014.
- Rajeswaran, A., Ghotra, S., Ravindran, B., and Levine, S. EPOpt: Learning robust neural network policies using model ensembles. *ICLR*, 2017.
- Rajeswaran, A., Mordatch, I., and Kumar, V. A game theoretic framework for model based reinforcement learning. In *International Conference on Machine Learning*, pp. 7953–7963. PMLR, 2020.
- Rigter, M., Lacerda, B., and Hawes, N. Risk-averse Bayes-adaptive reinforcement learning. *Advances in Neural Information Processing Systems*, 34:1142–1154, 2021.
- Rigter, M., Duckworth, P., Lacerda, B., and Hawes, N. Planning for risk-aversion and expected value in MDPs. *International Conference on Automated Planning and Scheduling*, 2022a.
- Rigter, M., Lacerda, B., and Hawes, N. RAMBO-RL: Robust adversarial model-based offline reinforcement learning. *Advances in Neural Information Processing Systems*, 2022b.
- Rockafellar, R. T. and Uryasev, S. Conditional value-at-risk for general loss distributions. *Journal of banking & finance*, 26(7):1443–1471, 2002.
- Ruszczynski, A. Risk-averse dynamic programming for Markov decision processes. *Mathematical programming*, 125(2):235–261, 2010.
- Shapiro, A., Dentcheva, D., and Ruszczyński, A. *Lectures on stochastic programming: modeling and theory*, chapter 5. SIAM, 2021a.
- Shapiro, A., Dentcheva, D., and Ruszczyński, A. *Lectures on stochastic programming: modeling and theory*, chapter 6. SIAM, 2021b.
- Sharma, A., Harrison, J., Tsao, M., and Pavone, M. Robust and adaptive planning under model uncertainty. In *Proceedings of the International Conference on Automated Planning and Scheduling*, volume 29, pp. 410–418, 2019.
- Sutton, R. S. Dyna, an integrated architecture for learning, planning, and reacting. *ACM Sigart Bulletin*, 2(4):160–163, 1991.
- Swazinna, P., Udluft, S., and Runkler, T. Overcoming model bias for robust offline deep reinforcement learning. *Engineering Applications of Artificial Intelligence*, 104: 104366, 2021.
- Tamar, A., Di Castro, D., and Mannor, S. Policy gradients with variance related risk criteria. *International Conference on Machine Learning*, 2012.
- Tamar, A., Chow, Y., Ghavamzadeh, M., and Mannor, S. Policy gradient for coherent risk measures. *Advances in Neural Information Processing Systems*, 28, 2015a.
- Tamar, A., Glassner, Y., and Mannor, S. Optimizing the CVaR via sampling. In *Twenty-Ninth AAAI Conference on Artificial Intelligence*, 2015b.
- Urpí, N. A., Curi, S., and Krause, A. Risk-averse offline reinforcement learning. *International Conference on Learning Representations*, 2021.
- Wang, J., Li, W., Jiang, H., Zhu, G., Li, S., and Zhang, C. Offline reinforcement learning with reverse model-based imagination. *Advances in Neural Information Processing Systems*, 34, 2021.
- Wang, S. S. A class of distortion operators for pricing financial and insurance risks. *Journal of risk and insurance*, pp. 15–36, 2000.
- Webster, S. R. and Flach, P. Risk sensitive model-based reinforcement learning using uncertainty guided planning. *arXiv preprint arXiv:2111.04972*, 2021.
- Wu, Y., Tucker, G., and Nachum, O. Behavior regularized offline reinforcement learning. *arXiv preprint arXiv:1911.11361*, 2019.
- Xie, T., Cheng, C.-A., Jiang, N., Mineiro, P., and Agarwal, A. Bellman-consistent pessimism for offline reinforcement learning. *Advances in Neural Information Processing Systems*, 34, 2021.

- Yang, R., Bai, C., Ma, X., Wang, Z., Zhang, C., and Han, L. RORL: Robust offline reinforcement learning via conservative smoothing. *Advances in Neural Information Processing Systems*, 2022.
- Yang, Y., Jiang, J., Zhou, T., Ma, J., and Shi, Y. Pareto policy pool for model-based offline reinforcement learning. In *International Conference on Learning Representations*, 2021.
- Yu, T., Thomas, G., Yu, L., Ermon, S., Zou, J. Y., Levine, S., Finn, C., and Ma, T. MOPO: Model-based offline policy optimization. *Advances in Neural Information Processing Systems*, 33:14129–14142, 2020.
- Yu, T., Kumar, A., Rafailov, R., Rajeswaran, A., Levine, S., and Finn, C. COMBO: Conservative offline model-based policy optimization. *Advances in neural information processing systems*, 34:28954–28967, 2021.
- Zhang, J., Cheung, B., Finn, C., Levine, S., and Jayaraman, D. Cautious adaptation for reinforcement learning in safety-critical settings. In *International Conference on Machine Learning*, pp. 11055–11065. PMLR, 2020.
- Zhou, G., Ke, L., Srinivasa, S., Gupta, A., Rajeswaran, A., and Kumar, V. Real world offline reinforcement learning with realistic data source. *arXiv preprint arXiv:2210.06479*, 2022.

# Appendices

## A. Risk Measures

In our experiments, we make use of two different risk measures in our algorithm: the conditional value at risk (CVaR) (Rockafellar & Uryasev, 2002), and the Wang risk measure (Wang, 2000). Here, we explain how the distribution over candidate successor states,  $s' \in \Psi$  is modified for these two risk measures in Algorithm 1. To avoid the need for excessive notation we assume that all sampled candidate successor states in  $\Psi$  are unique, and that no two successor states have exactly the same value, i.e.  $V(s'_i) \neq V(s'_j)$ , for any two different  $s'_i, s'_j \in \Psi$ .

**Conditional Value at Risk** Consider a probability space  $(\Omega, \mathcal{F}, P)$ , where  $\Omega$  is the sample space,  $\mathcal{F}$  is the event space, and  $P$  is a probability distribution over  $\mathcal{F}$ . For a continuous random variable  $Z$ , CVaR is the mean of the  $\alpha$ -portion of the worst outcomes:  $\rho_{\text{CVaR}}(Z, \alpha) = \mathbb{E}[z \sim Z \mid z \leq F_Z^{-1}(\alpha)]$ , where  $F_Z$  is the CDF of  $Z$ . For CVaR at confidence level  $\alpha$ , the corresponding risk envelope is:

$$\mathcal{B}_{\text{CVaR}_\alpha}(P) = \left\{ \xi : \xi(\omega) \in \left[0, \frac{1}{\alpha}\right] \forall \omega, \int_{\omega \in \Omega} \xi(\omega) P(\omega) d\omega = 1 \right\} \quad (10)$$

The risk envelope allows the likelihood for any outcome to be increased by at most  $1/\alpha$ . In Algorithm 1, for state-action pair  $(s, a)$ , we approximate the distribution over successor states as a discrete uniform distribution over candidate successor states  $s' \in \Psi$ , where  $\Psi$  is a set of  $m$  states sampled from  $\bar{T}(s, a, s')$ . This discrete distribution is  $\hat{T}(s, a, s') = \frac{1}{m}$  for all  $s' \in \Psi$ .

In Line 9 of Algorithm 1, we denote by  $\hat{\xi}^*$  the adversarial perturbation to the discrete transition distribution:

$$\hat{\xi}^* = \arg \min_{\xi \in \mathcal{B}_\rho(\hat{T}(s, a, \cdot))} \sum_{s' \in \Psi} \hat{T}(s, a, s') \cdot \xi(s') \cdot V^\pi(s')$$

Define  $\mathcal{V}_{s'}$  as the random variable representing the value of the successor state,  $V^\pi(s')$ , when the successor state is drawn from  $s' \sim \hat{T}(s, a, \cdot)$ . Also define the value at risk at confidence level  $\alpha \in (0, 1]$ , which is the  $\alpha$ -quantile of a distribution:  $\text{VaR}_\alpha(Z) = \min\{z \mid F_Z(z) \geq \alpha\}$ . Then, from the risk envelope in Equation 10, we can derive that the adversarial perturbation is:

$$\hat{\xi}_{\text{CVaR}}(s') \cdot \hat{T}(s, a, s') = \begin{cases} \frac{1}{m \cdot \alpha}, & \text{if } V(s') < \text{VaR}_\alpha(\mathcal{V}_{s'}). \\ 0, & \text{if } V(s') > \text{VaR}_\alpha(\mathcal{V}_{s'}). \\ 1 - \sum_{s' \in \Psi} \frac{1}{m \cdot \alpha} \mathbb{1}[V(s') < \text{VaR}_\alpha], & \text{if } V(s') = \text{VaR}_\alpha(\mathcal{V}_{s'}). \end{cases} \quad (11)$$

The last line of Equation 11 ensures that the perturbed distribution is a valid probability distribution (as required by the risk envelope in Equation 10).

**Wang Risk Measure** For parameter  $\eta$ , the Wang risk measure for random variable,  $Z$ , can be defined as the expectation under a distorted cumulative distribution function  $\rho_{\text{Wang}}(Z, \eta) = \int_{-\infty}^{\infty} z \frac{\partial}{\partial z} g(F_Z(z)) dz$ . The distortion function is  $g(\tau) = \Phi(\Phi^{-1}(\tau) + \eta)$ , where  $\Phi$  is the CDF of the standard normal distribution.

To compute the perturbation to  $\hat{T}(s, a, \cdot)$  according to the Wang risk measure, we order the candidate successor states according to their value. We use the subscript to indicate the ordering of  $s'_i$ , where  $V(s'_1) < V(s'_2) < V(s'_3) \dots < V(s'_m)$ . Then, the perturbed probability distribution is:

$$\hat{\xi}_{\text{Wang}}(s'_i) \cdot \hat{T}(s, a, s'_i) = \begin{cases} g\left(\frac{1}{m}\right), & \text{if } i = 1. \\ g\left(\frac{i}{m}\right) - g\left(\frac{i-1}{m}\right), & \text{if } 1 < i < m. \\ 1 - g\left(\frac{i-1}{m}\right), & \text{if } i = m. \end{cases} \quad (12)$$

The transition distribution perturbed according to the Wang risk measure assigns gradually decreasing probability to higher-value successor states. The parameter  $\eta$  controls the extent to which the probabilities are modified. For large  $\eta \gg 0$ , almost all of the probability is placed on the worst outcome(s), and as  $\eta \rightarrow 0$ , the perturbed distribution approaches a uniform distribution.

## B. Additional Results

### B.1. MuJoCo Stochastic Expected Value Results

Table 4: Expected value results for the Stochastic MuJoCo benchmarks using the normalisation procedure proposed by Fu et al. (2020). We report the normalised performance during the last 10 iterations of training averaged over 5 seeds.  $\pm$  captures the standard deviation over seeds. Highlighted numbers indicate results within 10% of the best score. “div.” indicates that the value function diverged for at least one run.

		1R2R <sub>CvaR</sub>	1R2R <sub>Wang</sub>	Ablation	O-RAAC	CODAC	RAMBO	CQL	IQL	TD3+BC
Medium	Hopper (Mod)	67.2 ± 5.7	65.9 ± 7.0	64.1 ± 10.0	15.6 ± 9.4	50.7 ± 3.0	72.9 ± 14.7	50.2 ± 0.6	50.6 ± 4.1	48.4 ± 1.4
	Walker2D (Mod)	67.3 ± 7.8	62.2 ± 6.3	27.6 ± 23.4	38.8 ± 7.1	44.1 ± 1.5	34.5 ± 2.2	58.4 ± 1.6	45.6 ± 1.3	41.4 ± 17.4
	Hopper (High)	57.1 ± 4.5	58.1 ± 5.9	53.0 ± 4.7	28.8 ± 11.0	69.9 ± 2.1	54.4 ± 4.4	74.7 ± 5.1	61.6 ± 8.0	66.3 ± 1.3
	Walker2D (High)	29.8 ± 11.8	58.8 ± 8.9	div.	41.6 ± 9.6	65.7 ± 0.6	56.9 ± 3.5	75.2 ± 1.3	54.8 ± 2.0	77.6 ± 2.3
Medium Replay	Hopper (Mod)	83.6 ± 18.6	76.8 ± 9.9	64.5 ± 9.8	15.8 ± 3.0	61.2 ± 10.7	67.6 ± 11.3	66.9 ± 10.8	-0.5 ± 0.0	38.2 ± 4.9
	Walker2D (Mod)	53.9 ± 9.4	51.7 ± 11.4	57.4 ± 3.0	24.2 ± 6.8	47.8 ± 19.7	63.6 ± 4.5	50.1 ± 1.9	16.2 ± 2.8	48.4 ± 1.5
	Hopper (High)	114.3 ± 10.8	102.0 ± 9.1	48.4 ± 16.0	26.2 ± 16.0	54.5 ± 2.9	54.1 ± 19.7	96.7 ± 13.0	15.1 ± 9.6	58.4 ± 6.1
	Walker2D (High)	84.1 ± 5.3	76.4 ± 6.0	75.4 ± 8.0	19.1 ± 4.7	80.4 ± 11.6	84.1 ± 4.0	61.1 ± 3.0	-0.1 ± 0.8	73.4 ± 2.3
Medium Expert	Hopper (Mod)	94.1 ± 17.2	71.3 ± 42.2	64.0 ± 41.7	32.8 ± 8.7	96.6 ± 8.8	71.9 ± 20.7	106.7 ± 3.8	107.5 ± 7.7	100.9 ± 2.0
	Walker2D (Mod)	72.2 ± 7.3	77.3 ± 9.1	div.	27.6 ± 12.4	81.7 ± 4.8	58.0 ± 22.3	94.2 ± 1.1	63.2 ± 1.7	93.5 ± 0.9
	Hopper (High)	54.1 ± 5.5	63.2 ± 11.0	48.4 ± 7.4	18.9 ± 11.2	79.9 ± 3.5	60.0 ± 6.1	88.3 ± 3.5	64.0 ± 16.5	89.9 ± 1.4
	Walker2D (High)	49.9 ± 15.4	44.4 ± 17.6	div.	27.3 ± 13.4	79.5 ± 18.0	31.1 ± 14.9	104.3 ± 2.3	72.7 ± 4.9	107.0 ± 2.3

### B.2. HIV Treatment Return Distributions

Figure 3 illustrates the return distributions for each algorithm from all evaluation episodes aggregated over 10 seeds per algorithm. Note that in the ablation in Figure 3c, training became unstable for a subset of the runs. This resulted in very poor performance for a subset of the runs. Because the plots in Figure 3 are aggregated across all 10 runs for each algorithm, this results in the strongly multi-modal performance observed for the ablation in Figure 3c.

## C. Implementation Details

The code for 1R2R will shortly be made publicly available. Please contact the lead author for details.

### C.1. Model Training

We represent the model as an ensemble of neural networks that output a Gaussian distribution over the next state and reward given the current state and action:

$$\widehat{T}_\phi(s', r|s, a) = \mathcal{N}(\mu_\phi(s, a), \Sigma_\phi(s, a)).$$

Following previous works (Yu et al., 2021; 2020; Rigter et al., 2022b), during model training we train an ensemble of 7 such dynamics models and pick the best 5 models based on the validation error on a held-out test set of 1000 transitions from the dataset  $\mathcal{D}$ . Each model in the ensemble is a 4-layer feedforward neural network with 200 hidden units per layer.  $P(T | \mathcal{D})$  is assumed to be a uniform distribution over the 5 models. Increasing the number of networks in the ensemble has been shown to improve uncertainty estimation (Lu et al., 2022). However, we used the same ensemble as previous works to facilitate a fair comparison.

The learning rate for the model training is 3e-4 for both the MLE pretraining, and it is trained using the Adam optimiser (Kingma & Ba, 2015). The hyperparameters used for model training are summarised in Table 5.

## C.2. Policy Training

We sample a batch of 256 transitions to train the policy and value function using soft actor-critic (SAC) (Haarnoja et al., 2018). We set the ratio of real data to  $f = 0.5$  for all datasets, meaning that we sample 50% of the batch transitions from  $\mathcal{D}$  and the remaining 50% from  $\widehat{\mathcal{D}}$ . We chose this value because we found it worked better than using 100% synthetic data (i.e.  $f = 0$ ), and it was found to work well in previous works (Yu et al., 2021; Rigter et al., 2022b). We represent the  $Q$ -networks and the policy as three layer neural networks with 256 hidden units per layer.

For SAC (Haarnoja et al., 2018) we use automatic entropy tuning, where the entropy target is set to the standard heuristic of  $-\dim(A)$ . The only hyperparameter that we modify from the standard implementation of SAC is the learning rate for the actor, which we set to  $1e-4$  as this was reported to work better in the CQL paper (Kumar et al., 2020) which also utilised SAC. For reference, the hyperparameters used for SAC are included in Table 5.

## C.3. 1R2R Implementation Details

When sampling successor states in Algorithm 1, we sample  $m = 10$  candidate successor states to generate the set  $\Psi$ . For each run, we perform 2,000 iterations of 1,000 gradient updates. The rollout policy used to generate synthetic data is the current policy. The base hyperparameter configuration for 1R2R that is shared across all runs is shown in Table 5.

The only parameters that we vary between datasets are the length of the synthetic rollouts ( $k$ ), and the risk measure parameter. Details are included in the Hyperparameter Tuning section below.

## C.4. 1R2R Hyperparameter Tuning

The hyperparameters that we tune for 1R2R are the length of the synthetic rollouts ( $k$ ), and the parameter associated with the chosen risk measure ( $\alpha$  for 1R2R<sub>CVaR</sub> or  $\eta$  for 1R2R<sub>Wang</sub>). For each dataset, we select the parameters that obtain the best online performance for the desired objective for that dataset. The objectives for each of the datasets are: optimising expected value for D4RL MuJoCo; optimising static CVaR<sub>0.1</sub> for Stochastic MuJoCo; and optimising static CVaR<sub>0.02</sub> for HIVTreatment.

The rollout length is tuned from  $k \in \{1, 5\}$ . For each of the two versions of our algorithm, 1R2R<sub>CVaR</sub> and 1R2R<sub>Wang</sub>, the parameters are tuned from the following settings:

- 1R2R<sub>CVaR</sub>: the rollout length,  $k$ , and CVaR parameter,  $\alpha$ , are selected from:  $(k, \alpha) \in \{1, 5\} \times \{0.5, 0.7, 0.9\}$ .
- 1R2R<sub>Wang</sub>: the rollout length,  $k$ , and Wang risk parameter,  $\eta$ , are selected from:  $(k, \eta) \in \{1, 5\} \times \{0.1, 0.5, 0.75\}$ .

Note that while the risk measures are only moderately risk-averse, in the dynamic risk approach of 1R2R, they are applied recursively at each step. This can result in a high degree of risk-aversion over many steps (Gagne & Dayan, 2021).

Please refer to Table 6 for a list of the hyperparameters used for 1R2R for each dataset, and to Table 5 for the base set of hyperparameters that is shared across all datasets.

# One Risk to Rule Them All

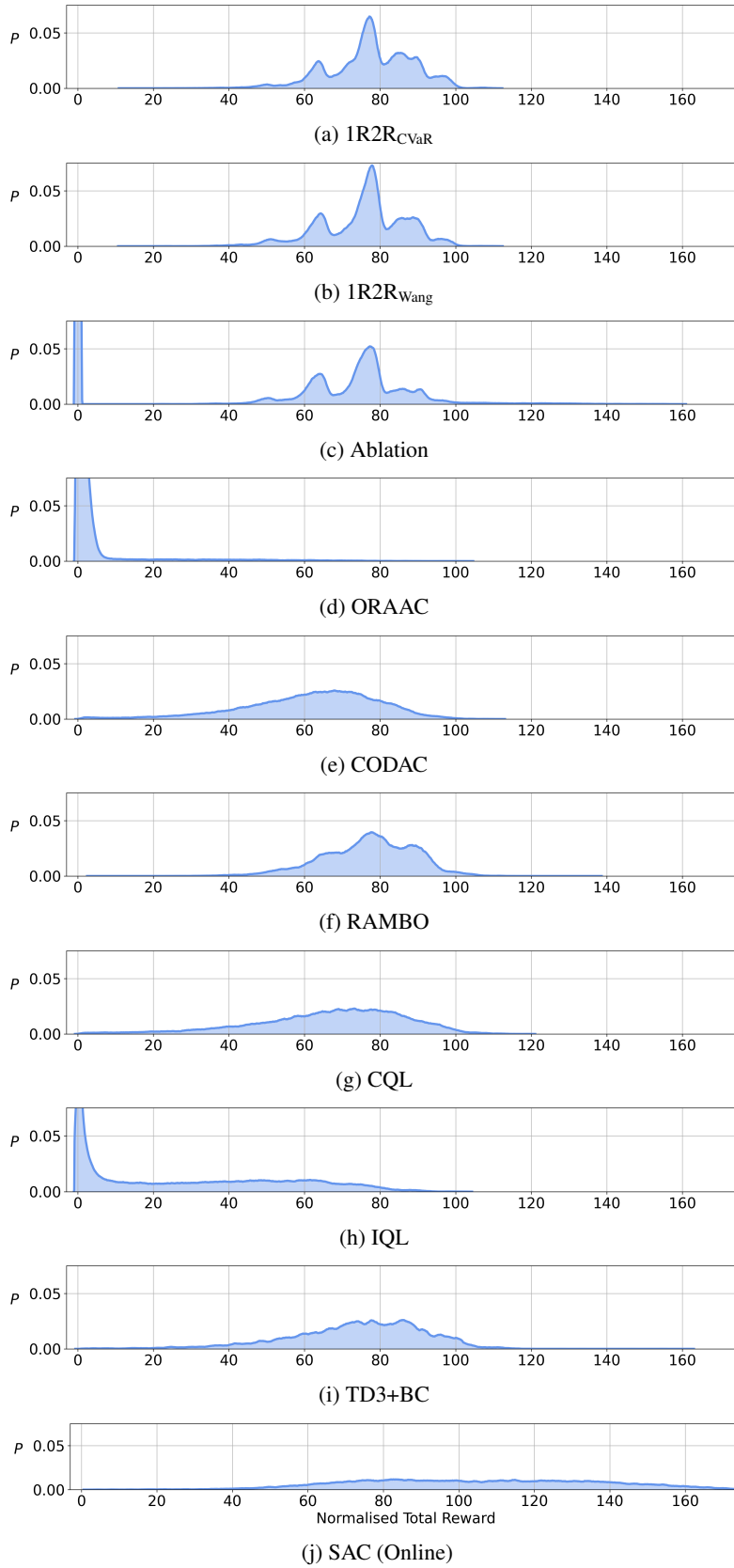


Figure 3: Return distributions for each algorithm on the HIV Treatment domain. The plots are generated by aggregating all evaluation episodes. There are 500 evaluation episodes per iteration for each of the last 10 iterations of training, across 10 seeds per algorithm, for a total of 50,000 evaluation episodes per plot.

Table 5: Base hyperparameter configuration shared across all runs of 1R2R.

	Hyperparameter	Value
SAC	critic learning rate	3e-4
	actor learning rate	1e-4
	discount factor ( $\gamma$ )	0.99
	soft update parameter ( $\tau$ )	5e-3
	target entropy	$-\dim(A)$
	batch size	256
1R2R	no. of model networks	7
	no. of elites	5
	ratio of real data ( $f$ )	0.5
	no. of iterations ( $N_{\text{iter}}$ )	2000
	no. of candidate successor states ( $m$ )	10
	rollout policy	current $\pi$

Table 6: Hyperparameters used by 1R2R for each dataset, chosen according to best online performance.  $k$  is the rollout length,  $\alpha$  is the parameter for CVaR, and  $\eta$  is the parameter for the Wang risk measure.

		1R2R (CVaR)		1R2R (Wang)	
		$k$	$\alpha$	$k$	$\eta$
Random	HalfCheetah	5	0.9	5	0.1
	Hopper	5	0.7	5	0.5
	Walker2D	5	0.9	5	0.1
Medium	HalfCheetah	5	0.9	5	0.1
	Hopper	5	0.9	5	0.1
	Walker2D	5	0.9	5	0.1
Medium Replay	HalfCheetah	5	0.9	5	0.1
	Hopper	1	0.5	1	0.75
	Walker2D	1	0.9	1	0.1
Medium Expert	HalfCheetah	5	0.9	5	0.1
	Hopper	5	0.9	5	0.1
	Walker2D	1	0.7	1	0.5
Medium	Hopper (Mod)	5	0.9	5	0.1
	Walker2D (Mod)	1	0.9	1	0.5
	Hopper (High)	5	0.9	5	0.1
	Walker2D (High)	1	0.7	1	0.1
Medium Replay	Hopper (Mod)	5	0.7	5	0.5
	Walker2D (Mod)	1	0.9	1	0.1
	Hopper (High)	5	0.5	5	0.75
	Walker2D (High)	1	0.9	1	0.1
Medium Expert	Hopper (Mod)	5	0.7	5	0.75
	Walker2D (Mod)	1	0.5	1	0.75
	Hopper (High)	5	0.9	5	0.5
	Walker2D (High)	1	0.7	1	0.5
HIVTreatment		1	0.7	1	0.5

## D. Experiment Details

### D.1. Computation Requirements

Each run of 1R2R requires 16-24 hours of computation time on a system with an Intel Core i7-8700 CPU @ 3.20GHz CPU and an NVIDIA GeForce GTX 1070 graphics card.

### D.2. Domains

The D4RL MuJoCo domains are from the D4RL offline RL benchmark (Fu et al., 2020). In this work, we introduce the following domains.

**Currency Exchange** This domain is an adaptation of the Optimal Liquidation Problem (Almgren & Chriss, 2001; Bao & Liu, 2019) to offline RL. We assume that the agent initially holds 100 units of currency A, and wishes to convert all of this to currency B before a deadline  $T$ , subject to an exchange rate which changes stochastically. At each time step, the agent may choose how much (if any) of currency A to convert to currency B at the current exchange rate.

An aggressive strategy is to delay converting the currency, in the hope that random fluctuations will lead to a more favourable exchange rate before the deadline  $T$ . However, this may lead to a poor outcome if the exchange rate decreases and fails to recover before the deadline. More risk-averse strategies are to either: a) gradually convert the currency over many steps, or b) immediately convert all of the currency even if the current exchange rate is mediocre, to avoid the risk of having to convert the money at even worse exchange rate in the future, to meet the deadline  $T$ .

The state space is 3-dimensional, consisting of: the timestep,  $t \in \{0, 1, 2, \dots, T\}$ ; the amount of currency A remaining,  $m \in [0, 100]$ ; and the current exchange rate,  $p \in [0, \infty)$ . We assume that the exchange rate evolves according to an Ornstein-Uhlenbeck process, which is commonly used for financial modelling (Maller et al., 2009):

$$dp_t = \theta(\mu - p_t)dt + \sigma dW_t, \tag{13}$$

where  $W_t$  denotes the Wiener process. In our implementation we set:  $\mu = 1.5$ ,  $\sigma = 0.2$ ,  $\theta = 0.05$ . The exchange rate at the initial time step is  $p_0 \sim \mathcal{N}(1, 0.05^2)$ . The action space is single dimensional,  $a \in [-1, 1]$ . We assume that a positive action corresponds to the proportion of  $m$  to convert to currency B at the current step, while a negative action corresponds to converting none of the currency. The reward is equal to the amount of currency B received at each step.

To generate the dataset, we generate data from a random policy that at each step chooses a uniform random proportion of currency to convert with probability 0.2, and converts none of the currency with probability 0.8.

**HIV Treatment** The environment is based on the implementation in Geramifard et al. (2015) of the physical model described by Ernst et al. (2006). The patient state is a 6-dimensional continuous vector representing the concentrations of different types of cells and viruses in the patients blood. There are two actions, corresponding to giving the patient Reverse Transcriptase Inhibitors (RTI) or Protease Inhibitors (PI) (or both). Unlike Ernst et al. (2006) which considered discrete actions, we modify the domain to allow for continuous actions representing variable quantities of each drug. Following previous work (Keramati et al., 2020), we assume that the treatment at each time step is applied for 20 days, and that there are 50 time steps. Therefore, each episode corresponds to a total period of 1000 days. Also following Keramati et al. (2020),

Table 7: Expected return received by a randomly initialised policy and an expert policy trained online using SAC. The expert SAC policy is trained online for 2e6 updates for the Stochastic MuJoCo domains, and 5e6 updates for HIVTreatment. In Tables 1, 2, and 3 the values reported are normalised between 0 and 100 using the procedure from Fu et al. (2020) and the values in this table.

	Random Policy	Expert Policy
Hopper (Moderate-Noise)	20.1	3049.4
Walker2D (Moderate-Noise)	-1.9	4479.2
Hopper (High-Noise)	11.2	2035.1
Walker2D (High-Noise)	-5.3	4101.3
HIVTreatment	-48.7	5557.9

we introduce stochasticity into the domain by adding noise to the efficacy of each drug ( $\epsilon_1$  and  $\epsilon_2$  in Ernst et al. (2006)). The noise added to the efficacy is normally distributed, with a standard deviation of 15% of the standard value.

For this domain, the dataset is constructed in the same manner as the *Medium-Replay* datasets from D4RL (Fu et al., 2020). Specifically, a policy is trained with SAC (Haarnoja et al., 2018) until it reaches  $\approx 40\%$  of the performance of an expert policy. The replay buffer of data collected until reaching this point is used as the offline dataset.

The reward function is that used by Geramifard et al. (2015), except that we scale the reward by dividing it by  $1e6$ . A low concentration of HIV viruses is rewarded, and a cost is associated with the magnitude of treatment applied, representing negative side effects. The average reward received by a random policy and an expert policy trained online using SAC (Haarnoja et al., 2018) can be found in Table 7. In the paper, values are normalised between 0 and 100 using the method proposed by Fu et al. (2020) and the values in Table 7. Thus, a score of 100 represents the average reward of an expert policy, and 0 represents the average reward of a random policy.

We assume that highly risk-averse decision making is desirable in this domain, to avoid some patients experiencing excessive hardship. Therefore, we assume that the objective is to optimise the static CVaR<sub>0.02</sub> (i.e. the average total reward in the worst 2% of runs).

**Stochastic MuJoCo** These benchmarks are obtained by applying random perturbation forces to the original *Hopper* and *Walker2D* MuJoCo domains. We chose to focus on these two domains as there is a risk of the robot falling over before the end of the episode. The perturbation forces represent disturbances due to strong wind or other sources of uncertainty. The force is applied in the  $x$ -direction at each step, according to a random walk on the interval  $[-f_{\text{MAX}}, f_{\text{MAX}}]$ . At each step, the change in force relative to the previous step is sampled uniformly from  $\Delta f \sim \text{Unif}(-0.1 \cdot f_{\text{MAX}}, 0.1 \cdot f_{\text{MAX}})$ . This is motivated by the fact that the strength of wind is often modelled as a random walk (Popko et al., 2016).

We test using two levels of noise applied. For the *Moderate-Noise* datasets, the level of noise results in a moderate degradation in the performance of an online SAC agent, compared to the original deterministic domain. For the *High-Noise* datasets, the level of noise results in a significant degradation in the performance of an online SAC agent. The value of  $f_{\text{MAX}}$  is set to the following in each of the domains:

- *Hopper Moderate-Noise*:  $f_{\text{MAX}} = 2.5$  Newtons.
- *Hopper High-Noise*:  $f_{\text{MAX}} = 5$  Newtons.
- *Walker2D Moderate-Noise*:  $f_{\text{MAX}} = 7$  Newtons.
- *Walker2D High-Noise*:  $f_{\text{MAX}} = 12$  Newtons.

We construct three datasets: *Medium*, *Medium-Replay*, and *Medium-Expert*. These are generated in the same manner as the D4RL datasets (Fu et al., 2020). The expert policy is a policy trained online using SAC until convergence. The medium policy is trained until it obtains  $\approx 40\%$  of the performance of the expert policy. The *Medium-Replay* dataset consists of the replay buffer collected while training the medium policy. The *Medium* dataset contains transitions collected from rolling out the medium policy. The *Medium-Expert* dataset contains a mixture of transitions generated by rolling out both the medium and the expert policy.

Following previous works (Urpí et al., 2021; Ma et al., 2021), we assume that the objective is to optimise the static CVaR<sub>0.1</sub> (i.e. the average total reward in the worst 10% of runs).

### D.3. Evaluation Procedure

For D4RL MuJoCo, we evaluate the policy for 10 episodes at each of the last 10 iterations of training, for each of 5 seeds. The average normalised total reward received throughout this evaluation is reported in the D4RL results table (Table 1).

For Stochastic MuJoCo, we evaluate the policy for 20 episodes at each of the last 10 iterations of training. CVaR<sub>0.1</sub> is computed by averaging the total reward in the worst two episodes at each iteration. The value of CVaR<sub>0.1</sub> is then averaged across the last 10 iterations, and across each of the 5 seeds. These are the results reported for CVaR<sub>0.1</sub> in Table 3.

For HIVTreatment and CurrencyExchange, we evaluate the policy for 500 episodes at each of the last 10 iterations of training, for each of 10 seeds. For HIVTreatment, CVaR<sub>0.02</sub> is computed by averaging the total reward in the worst 10 episodes at each evaluation. The value of CVaR<sub>0.02</sub> is then averaged across the last 10 iterations, and across each of the 10 seeds. All of the 50,000 evaluation episodes are aggregated together to generate the return distributions in Figures 2 and 3.

#### D.4. Baselines

We compare IR2R against offline RL algorithms designed for risk-sensitive optimisation (O-RAAC (Urpí et al., 2021) and CODAC (Ma et al., 2021)) in addition to performant risk-neutral model-based (RAMBO (Rigter et al., 2022b)) and model-free (IQL (Kostrikov et al., 2022), TD3+BC (Fujimoto & Gu, 2021), and CQL (Kumar et al., 2020)) algorithms.

For the baselines, we use the following implementations:

- O-RAAC: [github.com/nuria95/O-RAAC](https://github.com/nuria95/O-RAAC)
- CODAC: [github.com/JasonMa2016/CODAC](https://github.com/JasonMa2016/CODAC)
- RAMBO: [github.com/marc-rigter/rambo](https://github.com/marc-rigter/rambo)
- IQL: [github.com/ikostrikov/implicit\\_q\\_learning](https://github.com/ikostrikov/implicit_q_learning)
- TD3+BC: [github.com/sfujim/TD3\\_BC](https://github.com/sfujim/TD3_BC)
- CQL: [github.com/takuseno/d3rlpy](https://github.com/takuseno/d3rlpy)

The results for D4RL MuJoCo-v2 for RAMBO, IQL, and TD3+BC are taken from the original papers. Because the original CQL paper used the -v0 domains, we report the results for CQL on the -v2 domains from Wang et al. (2021). The results for CODAC in the original paper use D4RL MuJoCo-v0, and O-RAAC does not report results on the D4RL benchmarks. Therefore, we obtain the results for D4RL MuJoCo-v2 for CODAC and O-RAAC by running the algorithms ourselves. The results for all baseline algorithms for the other domains are obtained by running the algorithms ourselves.

#### D.5. Baseline Hyperparameter Tuning

We tune each of the algorithms online to achieve the best performance for the desired objective in each dataset. The desired optimisation objectives in each domain are: expected value in D4RL MuJoCo; static CVaR<sub>0.02</sub> in HIVTreatment; and static CVaR<sub>0.1</sub> in Stochastic MuJoCo. O-RAAC and CODAC can be configured to optimise a static risk measure, or expected value. Therefore, we set O-RAAC and CODAC to optimise the appropriate objective for each dataset.

For each of the baseline algorithms, we tune the following parameters based on the best online performance (averaged over 5 seeds for the MuJoCo domains, and 10 seeds for HIVTreatment) for the target objective. Where a hyperparameter value is not specified, it was set to the default value in the corresponding original paper.

- CODAC: The risk measure to optimise is set to the desired objective (Expected value/CVaR<sub>0.02</sub>/CVaR<sub>0.1</sub>). For Stochastic MuJoCo and HIVTreatment, we tune the parameters in the same manner as the original paper (Ma et al., 2021), choosing  $(\omega, \zeta) \in \{0.1, 1, 10\} \times \{-1, 10\}$ . For Stochastic MuJoCo and HIVTreatment we use the default critic learning rate of  $\eta_{critic} = 3e - 5$ . To generate the results for CODAC on D4RL MuJoCo-v2, we use the same parameters as reported in the paper for D4RL MuJoCo-v0.
- O-RAAC: The risk measure to optimise is set to the desired objective (Expected value/CVaR<sub>0.02</sub>/CVaR<sub>0.1</sub>). Following the original paper (Urpí et al., 2021) we tune the imitation learning weighting:  $\lambda \in \{0.25, 0.5\}$ .
- RAMBO: We tuned the rollout length and adversarial weighting from:  $(k, \lambda) \in \{(1, 3e - 4), (2, 3e - 4), (5, 3e - 4), (5, 0)\}$ . This is the same procedure as in the original paper (Rigter et al., 2022b), except that we additionally included a rollout length of 1 as we found this was necessary for RAMBO to train stably on some of the stochastic domains.
- IQL: For Stochastic MuJoCo, we used the same parameters as for D4RL MuJoCo in the original paper (Kostrikov et al., 2022). For HIVTreatment, we chose the best performance between the parameters for D4RL MuJoCo and D4RL AntMaze from the original paper.
- CQL: Following the original paper (Kumar et al., 2020), we tuned the Lagrange parameter,  $\tau \in \{5, 10\}$ . All other parameters are set to their default values.
- TD3+BC: Following the original paper, we set  $\alpha$  to 2.5 (Fujimoto & Gu, 2021).